Environmental Microbiology (2020) **22**(8), 3005–3019 doi:10.1111/1462-2920.15035

Minireview

The use of isothermal titration calorimetry to unravel chemotactic signalling mechanisms

Miguel A. Matilla, David Martín-Mora and Tino Krell*

Department of Environmental Protection, Estación Experimental del Zaidín, Consejo Superior de Investigaciones Científicas, Granada, Spain.

Summary

Chemotaxis is based on the action of chemosensory pathways and is typically initiated by the recognition of chemoeffectors at chemoreceptor ligand-binding domains (LBD). Chemosensory signalling is highly complex; aspect that is not only reflected in the intricate interaction between many signalling proteins but also in the fact that bacteria frequently possess multiple chemosensory pathways and often a large number of chemoreceptors, which are mostly of unknown function. We review here the usefulness of isothermal titration calorimetry (ITC) to study this complexity. ITC is the gold standard for studying binding processes due to its precision and sensitivity, as well as its capability to determine simultaneously the association equilibrium constant, enthalpy change and stoichiometry of binding. There is now evidence that members of all major LBD families can be produced as individual recombinant proteins that maintain their ligand-binding properties. High-throughput screening of these proteins using thermal shift assays offer interesting initial information on chemoreceptor ligands, providing the basis for microcalorimetric analyses and microbiological experimentation. ITC has permitted the identification and characterization of many chemoreceptors with novel specificities. This ITC-based approach can also be used to identify signal molecules that stimulate members of other families of sensor proteins.

Received 25 March, 2020; revised 20 April, 2020; accepted 21 April, 2020. *For correspondence. E-mail tino.krell@eez.csci.es; Tel. (+34) 958 181600; Fax (+34) 958 135740.

Introduction

Chemosensory pathways correspond to a major mechanism in bacterial signal transduction. Most chemosensory pathways mediate chemotaxis, whereas others are associated with type IV pili-based motility or the control of second messenger levels such as cAMP or c-di-GMP (Whitchurch *et al*., 2004; Hickman *et al*., 2005; Fulcher *et al*., 2010; Wuichet and Zhulin, 2010). The key element of a chemosensory pathway is the ternary complex formed by chemoreceptors, the CheW coupling protein and the CheA autokinase (Parkinson *et al*., 2015). Canonical chemoreceptors possess extracytoplasmic ligand-binding domains (LBD) and ligand recognition creates a molecular stimulus that is transduced across the membrane where it modulates CheA autophosphorylation, leading subsequently to changes in the transphosphorylation activity of the CheY response regulator (Fig. 1). The ratio of CheY to CheY-P defines the pathway output and, in the case of pathways that mediate chemotaxis, only CheY-P is able to bind to the flagellar motor altering its activity (Parkinson *et al*., 2015; Bi and Sourjik, 2018). Chemotaxis pathways are able to sense compound gradients and this capacity is primarily due to temporal adaptation mechanisms that adjust the pathway sensitivity to the present signal concentration. The primary adaptation mechanism consists in the methylation and demethylation of several glutamyl residues at the chemoreceptor signalling domain by the CheR methyltransferase and the CheB methylesterase respectively (Parkinson *et al*., 2015; Bi and Sourjik, 2018) (Fig. 1).

Chemosensory pathways represent complex signal transduction mechanisms and this complexity resides in different levels. First, a significant number of proteins participate in chemosensory signalling. Next to the six core proteins mentioned above, additional proteins were identified that are present in some but not all pathways, as exemplified by the CheD deamidase, the CheW-REC domain fusion protein CheV or the CheC, CheZ and CheX phosphatases (Wuichet and Zhulin, 2010). Furthermore, the scientific community keeps identifying additional proteins that participate in some signalling cascades (Lertsethtakarn *et al*., 2015; Xu *et al*., 2016;

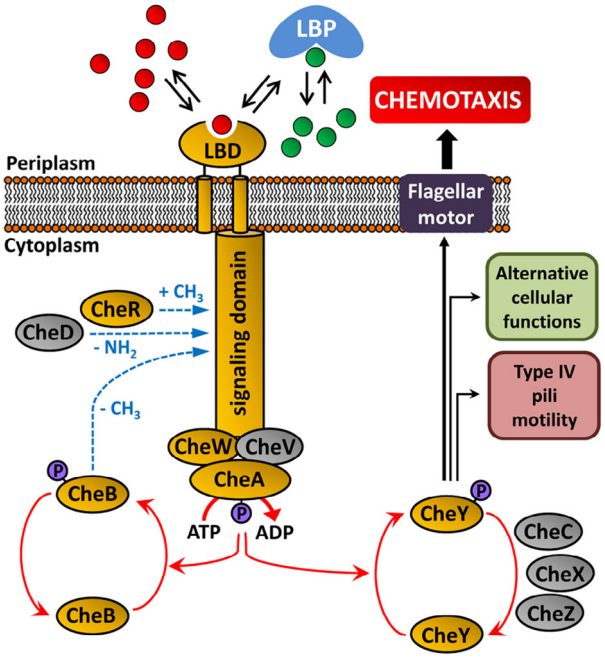

Fig 1 Schematic representation of a chemosensory pathway. Core proteins, present in almost all chemosensory pathways, are shown in yellow, whereas auxiliary proteins, present in only some pathways, are coloured in grey. Phosphorylation processes are shown by red arrows and methylation, demethylation and deamidation by blue arrows. Signal molecules are shown by red and green spheres. LBD: ligand binding domain; LBP: ligand binding protein. [Color figure can be viewed at wileyonlinelibrary.com]

Du *et al*., 2018). The second level of complexity lies in the fact that bacteria frequently have multiple pathways that are composed of homologous signalling proteins. For example, *Myxococcus xanthus* and *Pseudomonas aeruginosa* possess eight and four pathways respectively (Zusman *et al*., 2007; Ortega *et al*., 2017b). However, it remains to be established to what degree these pathways are insulated or whether there is cross-talk among them. The third level of intricacy is the elevated number of chemoreceptors encoded in the genomes of many bacteria that, in some cases, can reach 80 (Bardy *et al*., 2017; Gumerov *et al*., 2020). The large majority of chemoreceptors are of unknown function and their identification represents a major research need (Martin-Mora *et al*., 2018b). Furthermore, many chemoreceptor genes are not associated with signalling genes and a current challenge resides in identifying which receptor stimulates which pathway (Briegel *et al*., 2016; Jones and Armitage, 2017; Ortega *et al*., 2017b). There is also evidence that LBDs evolve rapidly causing a significant sequence divergence (Gavira *et al*., 2020), which in turn hampers the functional annotation of chemoreceptors by homology. Therefore, experimental approaches are required for the identification of chemoreceptor ligands and function.

Isothermal titration calorimetry (ITC) is based on the detection of heat changes that arise from the molecular interaction of two molecules. In a typical experiment, a macromolecule solution is titrated with a ligand solution and the resulting thermogram is corrected using the heats that are generated by the injection of ligand into buffer. ITC has become the gold-standard technique for studying binding processes due to its high precision, sensitivity and its capability for the simultaneous determination of the association equilibrium constant as well as the enthalpy change and stoichiometry of binding (Krell, 2008; Ladbury, 2010; Vega *et al*., 2015). In contrast to other techniques, both ligands are in solution and do not require modification or immobilization. A reliable determination of the K_D from a single ITC experiment is typically limited to the range 100 μM to 1 nM (Krainer and Keller, 2015). ITC is not suited to study ultra-tight binding interactions. A requisite for the study of tight ligand binding is the presence of at least two points at the fast rising part of the titration curve, necessary to define the equilibrium. In case only a single point is observed, it can be concluded that binding occurs with ultra-tight affinity but 'equilibrium constants' provided by the analysis software are not valid. In those cases, the K_D can be assessed indirectly by competition or displacement assays, provided that a suitable competitive ligand is available, whose K_D falls within the directly accessible window (Velazquez-Campoy and Freire, 2006; Krainer and Keller, 2015). ITC stands out for its universality since there are almost no limitations as to the nature of ligands that can be analysed or the choice of the analysis buffer and temperature. Particularly over the last 10 years, ITC analyses have permitted to significantly advance our knowledge on chemoreceptors and chemosensory pathways. In this review, we aim at summarizing this work putting particular emphasis on the usefulness of ITC in the identification and characterization of novel chemoreceptors.

Understanding CheR function

Product feedback inhibition and assessment of allostericity

CheR is one of the core signalling proteins of a chemosensory pathway and is present in almost all pathways (Wuichet and Zhulin, 2010). The substrate and product of the CheR-catalysed reaction are S-adenosylmethionine (SAM) and S-adenosylhomocysteine (SAH) respectively. Early studies of *Salmonella typhimurium* CheR have shown that SAH binds tighter than SAM to the same site at CheR (Simms and Subbaramaiah, 1991), indicative of product feedback inhibition. Microcalorimetric studies of the three and, respectively, four CheR homologues of *Pseudomonas putida* KT2440

(Garcia-Fontana *et al*., 2013) and *P. aeruginosa* PAO1 (Garcia-Fontana *et al*., 2014) showed that in all cases SAH binding occurred with higher affinity than SAM (Fig. 2), suggesting that product feedback inhibition is a general characteristic of CheR enzymes. However, significant differences existed in the ratios of SAH/SAM binding constants, indicating different magnitudes of SAH-dependent inhibition among CheR homologues (Garcia-Fontana *et al*., 2013; Garcia-Fontana *et al*., 2014). So far, it has not been studied whether and to which degree alterations of the cellular SAH/SAM levels interfere with chemosensory signalling. However, data available do not preclude the possibility that the differential product feedback observed for the *Pseudomonas* CheR homologues may have a physiological significance.

Approximately 10% of chemoreceptors, including the model receptors Tar and Tsr, contain a C-terminal pentapeptide that is tethered to the C-terminus via an unstructured linker (Perez and Stock, 2007; Bartelli and Hazelbauer, 2011). This pentapeptide forms an additional binding site for CheR and CheB (Wu *et al*., 1996; Barnakov *et al*., 1999). However, its relevance is poorly understood since the removal of this pentapeptide from Tar resulted in receptor inactivation (Li and Hazelbauer, 2006), whereas many other chemoreceptors do not require this pentapeptide for correct function (Matilla and Krell, 2017). ITC experiments showed that *Escherichia coli* and *S. typhimurium* CheR bound this pentapeptide (NWETF) with K_D values of approx. 2 μM (Wu *et al*., 1996) and 10 μM (Yi and Weis, 2002). Similar microcalorimetric titrations using the pentapeptide from the McpB (synonym Aer2) chemoreceptor of *P. aeruginosa* resulted in a K_D of 0.5 μM (Garcia-Fontana *et al*., 2014). Data thus indicate that CheR binds much tighter to the pentapeptide binding site as compared to the binding site covering the methylation sites for which a K_D of 120–200 μM had been determined (Li and Hazelbauer, 2020).

One possibility to explain the relevance of this additional CheR binding site is a potential allostericity between the pentapeptide and substrate/product binding sites at CheR, a question that had been addressed using ITC. In initial experiments, CheR of *S. typhimurium* (Yi and Weis, 2002) and $CheR_2$ from *P. aeruginosa* (Garcia-Fontana *et al*., 2014) were titrated with either pentapeptide, SAM or SAH. These experiments were then repeated in the presence of saturating concentrations of a ligand that binds to the other binding site. Both studies unequivocally concluded that there is no allostericity between both sites, providing further support to the view that pentapeptide binding mainly serves to localize CheR proteins close to the chemoreceptor methylation sites (Wu *et al*., 1996).

Specificity of CheR homologues for chemoreceptors

Pseudomonas aeruginosa contains a single chemoreceptor with a C-terminal pentapeptide, McpB (or Aer2), and four CheR homologues (Garcia-Fontana *et al*., 2014). The question is thus whether a single or multiple CheR homologues interact with this pentapeptide. The microcalorimetric titration of the four purified CheRs showed that exclusively $CheR_2$, but not any of the remaining three

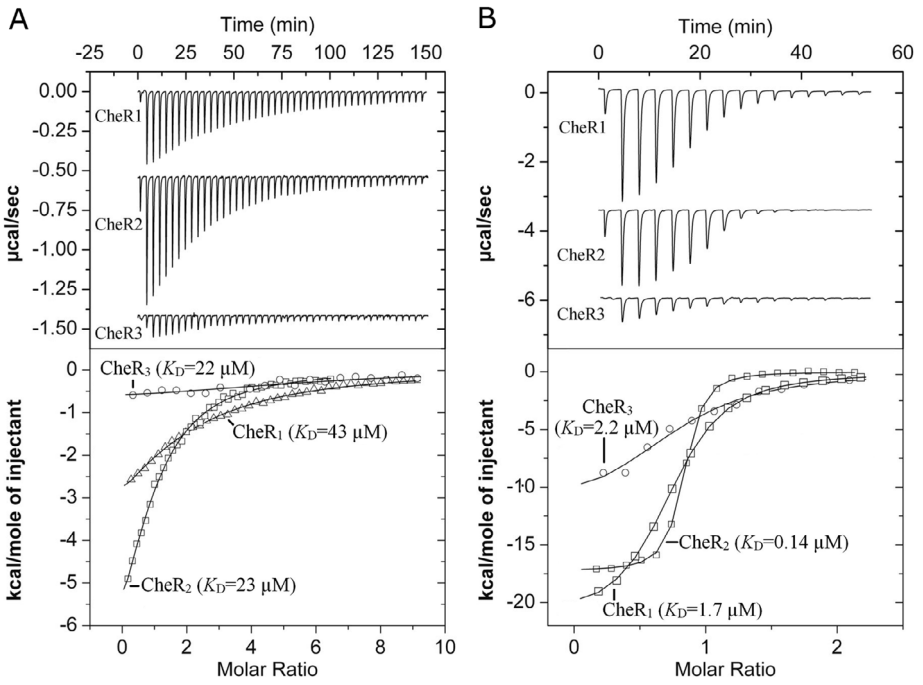

Fig 2 Titration of the three CheR homologues of P. putida KT2440 with S-adenosylmethionine (A) and S-adenosylhomocysteine (B). Upper panel: Raw titration data; lower panel: integrated, concentration-normalized and dilution heat corrected titration data. The lines are best fits with a model for the binding of a single ligand to a macromolecule. The corresponding dissociation constants are indicated. Modified version of figure reproduced with permission from Garcia-Fontana *et al*. (2013).

CheR homologues, recognized this pentapeptide (Fig. 3) (Garcia-Fontana *et al*., 2014). What is thus the sequence or structural property of $CheR_2$ that can be associated with pentapeptide recognition? An alignment of pentapeptide-dependent and independent CheR sequences revealed the presence of a three amino acid insert that was exclusively present in pentapeptide-dependent enzymes and that was located to the pentapeptide binding site (Perez and Stock, 2007; Garcia-Fontana *et al*., 2014). Microcalorimetric titrations of a CheR mutant from which this insert had been removed showed an absence of pentapeptide binding and this three amino acid insert can thus be used to predict the capacity of CheR enzymes to bind to pentapeptides (Garcia-Fontana *et al*., 2014). Further experiments revealed that exclusively $CheR_2$ methylates the pentapeptide-containing receptor McpB and that the removal of the pentapeptide from the receptor abolished $CheR_2$ binding and methylation (Garcia-Fontana *et al*., 2014). Microcalorimetry hence played a central role in establishing that the presence of this pentapeptide permits the targeting of a specific receptor by a specific methyltransferase. Interestingly, the presence of terminal pentapeptides is highly conserved in the family of McpB (Aer2) like chemoreceptors (Ortega *et al*., 2020).

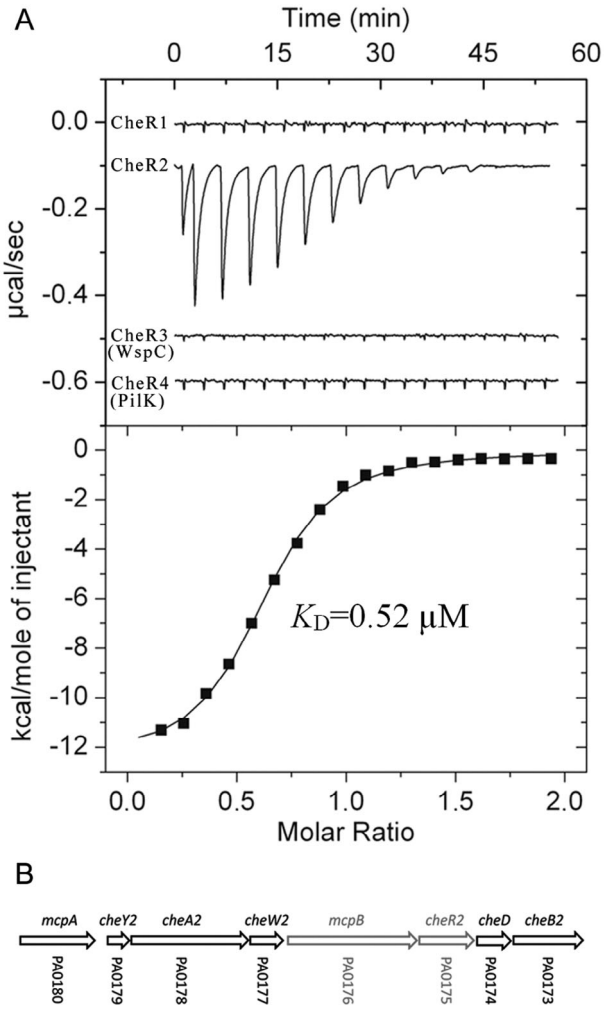

Fig 3 Specificity of recognition of $CheR_2$ by McpB. A. Microcalorimetric titration of the four CheR homologues from *P. aeruginosa* PAO1 with the C-terminal pentapeptide (GWEEF) from the McpB chemoreceptor. B. Organization of the *che2* gene cluster in *P. aeruginosa* PAO1. The genes conceding the proteins that specifically interact are shown in grey. Reproduced with permission from Garcia-Fontana *et al*. (2014).

Characterization of the c-di-GMP-mediated regulatory mechanisms

The c-di-GMP second messenger is a central signal molecule that controls motility and chemotaxis at the transcriptional and post-transcriptional level (Jenal *et al*., 2017). The precise determination of c-di-GMP dissociation constants provide initial insight at which effector concentration responses are generated.

In *E. coli*, the PilZ domain-containing protein YcgR responds to c-di-GMP by reducing swimming speed and chemotaxis by acting as a flagellar brake through its direct interaction with different components of the flagellar motor (Paul *et al*., 2010; Hou *et al*., 2020). ITC studies showed that YcgR binds c-di-GMP with a K_D of 141 nM (Hou *et al*., 2020) and fluorescence resonance transfer (FRET) assays revealed a strong interaction between YcgR and the flagellar stator protein MotA only in the presence of c-di-GMP (Boehm *et al*., 2010). A recent high-throughput screening in *E. coli* identified the deacetylase CobB as a novel c-di-GMP binding protein. CobB was shown to modulate chemotaxis by deacetylating the response regulator CheY (Li *et al*., 2010) and further studies demonstrated that c-di-GMP binding to CobB inhibits its deacetylation activity of the protein (Xu *et al*., 2019). ITC studies showed that CobB binds this second messenger with much lower affinity (K_D of 4.7 µM) (Xu *et al*., 2019), indicating that its regulatory effects sets in at comparatively higher c-di-GMP levels.

In *P. aeruginosa*, the c-di-GMP responsive transcriptional regulator FleQ plays a key role in this regulatory mechanism and an initial measurements using labelled c-di-GMP resulted in an apparent K_D for FleQ binding in the range of 10–25 µM (Hickman and Harwood, 2008). However, microcalorimetric titrations have permitted to precisely determine the K_D to be 7.2 µM (Baraquet and Harwood, 2013). MapZ is another c-di-GMP responsive protein of *P. aeruginosa* that regulates chemotaxis at the post-transcriptional level. In its c-di-GMP bound form, it binds to $CheR_1$ inhibiting chemoreceptor methylation (Xu *et al*., 2016). Microcalorimetric titrations determined the K_D of the c-di-GMP interaction with MapZ to be 8.8 µM (Xu *et al*., 2016). The proximities of the

dissociation constants for binding of c-di-GMP to FleQ and MapZ thus suggest that the cellular onset of c-di-GMP-mediated regulatory processes at the transcriptional and post-transcriptional level occur almost simultaneously. Furthermore, a K_D of c-di-GMP saturated MapZ for $CheR_1$ of 29 nM was reported by ITC (Yan *et al*., 2018), indicating that c-di-GMP recognition by MapZ is the rate-limiting step in this regulatory process.

Chemoreceptors

Ligand-binding studies to full-length receptors

Very interesting insight was obtained from microcalorimetric titrations of full-length Tsr, either solubilized in detergent micelles or inserted into the membrane, with its ligand serine (Lin *et al*., 1994). An *n*-value of 0.5 was obtained for the detergent solubilized sample, which is consistent with the binding of one ligand to the receptor dimer. In the membrane inserted Tsr, a condition under which chemoreceptors pack into arrays (Briegel *et al*., 2012), this value was lower indicating that not all binding sites are accessible; probably due to the steric hindrance imposed by the proximity of receptors in the array. The authors determined a K_D of approximately 25 μM for serine binding to the full-length receptor (Lin *et al*., 1994) that was similar to the value of 35 μM as reported by microcalorimetric titration of the individual Tsr LBD (Tajima *et al*., 2011). These results thus demonstrated that the molecular features for ligand recognition are present in the individual LBD, validating in turn approaches using the individual domains that are discussed below.

Ligand-binding studies to individual ligand-binding domains

The majority of chemoreceptors are of unknown function and their identification forms the basis for understanding the forces that have led to the evolution of chemoreceptors in a particular ecological habitat. The purification of significant amounts of full-length receptors is still a labour-intensive undertaking since it requires detergent-mediated protein extraction from the membrane. Data primarily available for Tar and Tsr show that the binding affinities of ligands to the full-length protein (Clarke and Koshland, 1979; Lin *et al*., 1994; Bjorkman *et al*., 2001) and to the individual LBD (Milligan and Koshland, 1993; Tajima *et al*., 2011) are comparable. There is now evidence that LBDs of all major families can be produced as individual, soluble and folded protein, and Table 1 lists the articles that report microcalorimetric titrations of recombinant chemoreceptor LBDs with chemoeffectors. The individual LBDs can generally be produced in significant amounts in a one-step purification process using affinity chromatography. In initial studies, the microcalorimetric titration of individual LBDs with ligands was used to characterize signal binding to chemoreceptors that were identified by a phenotypic analysis of mutants (Glekas *et al*., 2010; Lacal *et al*., 2010). However, the identification of chemoreceptor function by screening chemoreceptor mutants is not always successful, which is due to the fact that many bacteria possess multiple chemoreceptors with overlapping ligand specificities, to the masking of chemotaxis by energy tactic mechanisms or as a consequence of the insufficient receptor expression under the experimental conditions used (Alvarez-Ortega and Harwood, 2007; Ni *et al*., 2013; Parales *et al*., 2013; Ni *et al*., 2015).

Identification of novel chemoreceptors by the combined use of thermal shift assays and ITC. A powerful approach that has accelerated the identification of novel chemoreceptors consists in the combined use of thermal shift assays (TSA) and isothermal titration calorimetry (McKellar *et al*., 2015; Fernández *et al*., 2016; Martin-Mora *et al*., 2018b). Ligand binding to proteins does typically increase the T_m value or the midpoint of protein unfolding transition (Chiu and Prenner, 2011). The T_m value corresponds approximately to the temperature at which half the protein is in its native conformation, whereas the remaining half has undergone thermal unfolding. Commercially available ligand collections can thus be screened for compounds that increase the T_m of the individual LBDs. This assay can be conducted in high-throughput format using 96-well plates. Further technical detail on this assay can be found in the study by Ehrhardt *et al*. (2018) and Fernandez *et al*. (2018). Typically, T_m shifts superior to 2°C are considered significant and ITC studies are conducted to confirm ligand binding as well as to determine the thermodynamic parameters of the interaction. This combined TSA-ITC approach has resulted in the identification and characterization of a number of receptors with novel ligand specificities of which some are listed below.

- *Polyamines and histamine.* TSA-based ligand screening has led to the identification of two homologous receptors, TlpQ and McpU, in *P. aeruginosa* PAO1 and *P. putida* KT2440, respectively, that recognize the polyamines putrescine, cadaverine, spermidine, agmatine, ethylenediamine as well as histamine (Corral-Lugo *et al*., 2016; Corral-Lugo *et al*., 2018). The LBDs of both receptors share 62% sequence identity and, although both receptors possess the same ligand spectrum, ligands bind much tighter to TlpQ-LBD. The latter domain is so far the only LBD that binds five different ligands with nanomolar affinities and the K_D of 56 nM for spermidine is the highest affinity for

Table 1 Dissociation constants for the binding of chemoeffectors to recombinant ligand binding domains of chemoreceptors as determined by ITC.

Receptor	LBD type	Species	Chemoeffector	K_D (μM) range	References
McpH	dCACHE	*Pseudomonas putida* KT2440	Metabolizable purines	1.3–4.3	Fernandez *et al*. (2016)
McpG	dCACHE	*P. putida* KT2440	γ-aminobutyrate (GABA)	0.175	Reyes-Darias *et al*. (2015b)
McpU	dCACHE	*P. putida* KT2440	Polyamines, histamine	0.48–39	Corral-Lugo *et al*. (2016) and Corral-Lugo *et al*. (2018)
McpA	dCACHE	*P. putida* KT2440	12 l-amino acids	0.6–373	Corral-Lugo *et al*. (2016)
TlpQ	dCACHE	*P. aeruginosa* PAO1	Polyamines, histamine	0.056–1.7	Corral-Lugo *et al*. (2018)
PctA	dCACHE	*P. aeruginosa* PAO1	17 l-amino acids	0.28–116	Rico-Jimenez *et al*. (2013)
PctB	dCACHE	*P. aeruginosa* PAO1	5 l-amino acids	1.2–1096	Rico-Jimenez *et al*. (2013)
PctC	dCACHE	*P. aeruginosa* PAO1	GABA, 2 l-amino acids	1.2–80	Rico-Jimenez *et al*. (2013)
CtaA	dCACHE	*P. fluorescens* Pf0-1	7 l-amino acids	4.7–447	(Ud-Din *et al*., 2020)
McpX	dCACHE	*Sinorhizobium meliloti RU11*/001	Quaternary ammonium compounds, L-Pro	0.138–2300	Webb *et al*. (2017b)
McpU	dCACHE	*S. meliloti RU11*/001	L-Pro[aa]	104	(Webb *et al*., 2014)
McpC	dCACHE	*Bacillus subtilis* OI1085	12 l-amino acids	14–3700	Glekas *et al*. (2012)
McpB	dCACHE	*B. subtilis* OI1085	L-Asn[bb]	14	Glekas *et al*. (2010)
Mlp24	dCACHE	*Vibrio cholerae* O395N1	10 l-amino acids, calcium ions[cc]	4.7–452.5	Nishiyama *et al*. (2012) and Takahashi *et al*. (2019)
Mlp37	dCACHE	*V. cholerae* O395N1	Taurine, 3 l-amino acids[dd]	2.7–5.6	Nishiyama *et al*. (2016))
Psa-PscA	dCACHE	*P. syringae* pv. *actinidiae*	D/L-Asp, L-Glu	2.3–27	McKellar *et al*. (2015))
Psto-PscA	dCACHE	*P. syringae* pv. tomato	D/L-Asp, L-Glu	1.2–3.4	Cerna-Vargas *et al*. (2019)
McpA	dCACHE	*B. amyloliquefaciens* SQR9	Asp, citric acid[ee]	0.24–0.39	Feng *et al*. (2018)
McpB	dCACHE	*B. amyloliquefaciens* SQR9	Sodium decanoate[ee]	3.4	Feng *et al*. (2018)
McpC	dCACHE	*B. amyloliquefaciens* SQR9	Amino acids[ee]	3.62–3.64	Feng *et al*. (2018)
TlpB	dCACHE	*B. amyloliquefaciens* SQR9	Phe, pentadecanoic acid[ee]	3.0–3.2	Feng *et al*. (2018)
Tlp3	dCACHE	*Campylobacter jejuni* NCTC 11168	L-Ile[ff]	86	Liu *et al*. (2015)
TlpC	dCACHE	*Helicobacter pylori* PMSS1	L-Lactate[gg]	155	Machuca *et al*. (2017)
McpP	sCACHE	*P. putida* KT2440	C2/C3-carboxylic acids	34–107	Garcia *et al*. (2015)
PA2652	sCACHE	*P. aeruginosa* PAO1	C4-dicarboxylic acids	23–1240	Martin-Mora *et al*. (2018a)
PscD	sCACHE	*P. syringae* pv. *actinidiae*	C2/C3-carboxylic acids	23–356	Brewster *et al*. (2016)
McpV	sCACHE	*S. meliloti RU11*/001	C2/C3/C4-carboxylic acids	3.4–280	Compton *et al*. (2018)
Tar	4HB	*Escherichia coli* K12	Asp and derivatives	0.54–268	Tajima *et al*. (2011) and Bi *et al*. (2013)
Tsr	4HB	*E. coli* K12	L-Ser	36	Takahashi *et al*. (2019)
PcaY_PP	4HB	*P. putida* KT2440	Cyclic carboxylic acids	3.7–138	Fernandez *et al*. (2017)
CtpH	4HB	*P. aeruginosa* PAO1	Pi, compounds with *pyrophosphate moiety*	22–103	Rico-Jimenez *et al*. (2016)
McpB	4HB	*Ralstonia pseudosolanacearum* Ps29	Boric acid	5.4	Hida *et al*. (2017)
MCP2201	4HB	*Comamonas testosteroni* CNB-1	TCA cycle intermediates	18–378	Ni *et al*. (2013)
MCP2983	4HB	*C. testosteroni* CNB-1	*Cis*-aconitate	6.6 and 152.7[hh]	Ni *et al*. (2015)
MCP2901	4HB	*C. testosteroni* CNB-1	Citrate, aromatic hydrocarbons	19.6–1300	Huang *et al*. (2016)
McpR	not annotated	*B. amyloliquefaciens* SQR9	Arg	8.4[gg]	Feng *et al*. (2018)
McpS	HBM	*P. putida* KT2440	TCA cycle intermediates, butyrate, acetate	8.5–574	Lacal *et al*. (2010), Lacal *et al*. (2011), and Pineda-Molina *et al*. (2012)
McpQ	HBM	*P. putida* KT2440	Citrate, citrate/metal ion complexes	14–39	Martin-Mora *et al*. (2016a)
McpK	HBM	*P. aeruginosa* PAO1	α-Ketoglutarate	301 and 81[hh]	Martin-Mora *et al*. (2016b)
McpN	PilJ	*P. aeruginosa* PAO1	Nitrate	47	Martin-Mora *et al*. (2019)

[a]Fluorescence spectroscopy (Webb *et al*., 2017a) revealed binding of different L-amino acids.
[b]McpB also mediates chemotaxis to Asp, Glu and His (Hanlon and Ordal, 1994), but ITC assays have not been conducted.
[c]Calcium ion binding enhances affinity for amino acids.
[d]Mlp37 also mediates taxis toward Cys, Asp, Thr, Lys, Val and Gly (Nishiyama *et al*., 2016), but ITC assays have not been conducted.
[e]McpA, McpB, McpC and TlpB mediate chemotaxis to a wide range of compounds (Feng *et al*., 2018) and only some were used for ITC.
[f]Binding of nine additional compounds to Tlp3 was confirmed by surface plasmon and nuclear magnetic resonance (Rahman *et al*., 2014).
[g]Ligand range of the chemoreceptor has not been explored.
[h]Binding with cooperativity, given are K_{D1} and K_{D2}, respectively.

a chemoreceptor ligand so far measured (Fig. 4). Notably, in agreement with the high affinity for some of the TlpQ ligands, the onset of chemotactic response was with 500 nM very low (Corral-Lugo *et al*., 2018).

• *Nitrate.* The identification of the first chemoreceptor for nitrate illustrates well the usefulness of protein-based screening in the functional characterization of chemoreceptors. TSA and ITC revealed that McpN-LBD of

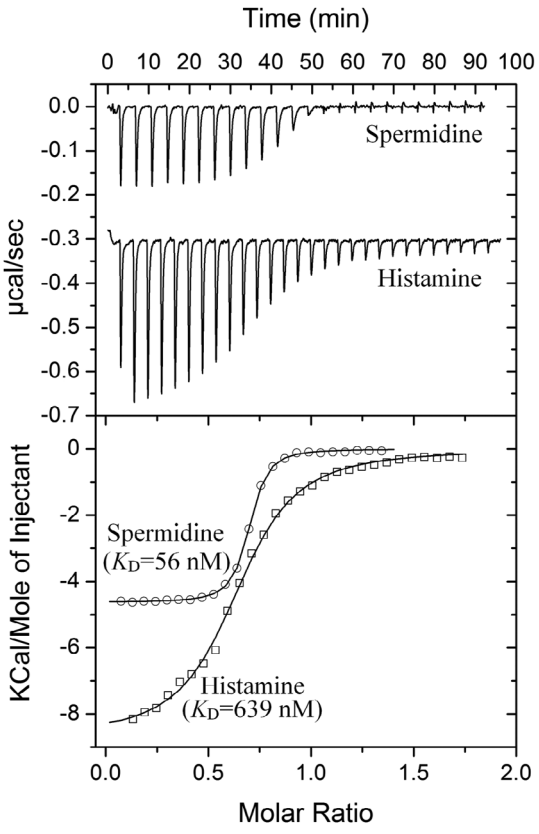

Fig 4 Microcalorimetric titration of the LBD of the *P. aeruginosa* PAO1 TlpQ chemoreceptor with histamine and spermidine. Data were published by Corral-Lugo *et al*. (2018).

P. aeruginosa PAO1 binds specifically nitrate (Martin-Mora *et al*., 2019), but chemotaxis experiments conducted under standard conditions did not provide any evidence for nitrate chemotaxis of the wild-type strain. However, the knowledge that there is a chemoreceptor that specifically binds nitrate and that was predicted to feed into the chemotaxis pathway (Ortega *et al*., 2017b) encouraged experimentation to identify the growth conditions under which nitrate chemotaxis may be observed. This research revealed that nitrate taxis in PAO1 is only observed under nitrate starvation conditions, which is likely to be due to the fact that the presence of nitrate largely reduced *mcpN* transcript levels (Martin-Mora *et al*., 2019).

• *Purines.* TSAs with the LBD of the *P. putida* KT2440 chemoreceptor McpH revealed T_m increases for adenine, guanine, xanthine and uric acid, which are all purine derivatives. In addition, subsequent ITC screening revealed binding to purine and the purine derivative hypoxanthine (Fernandez *et al*., 2016). Remarkably, although these ligands differ in structure, their affinities for McpH-LBD were highly similar (K_D = 1.3–4.3 µM), indicative of a plasticity in molecular recognition. These compounds form part of the purine degradation pathway that ultimately leads to urea, which serves as sole nitrogen source for KT2440 growth (Fernandez *et al*., 2016). In contrast, naturally occurring purine derivatives that are of no apparent metabolic value, namely caffeine, theophylline and theobromine, showed no binding to McpH-LBD, suggesting that the metabolic value was a force that has shaped the evolution of this receptor (Fernandez *et al*., 2016).

• *α-Ketoglutarate.* A number of compounds increased the T_m of McpK-LBD of *P. aeruginosa* PAO1, however, microcalorimetric studies showed that only α-ketoglutarate (αKG) showed binding (Martin-Mora *et al*., 2016b). Interestingly, the binding curve was biphasic and data analysis revealed binding with positive cooperativity, that contrasts with the negative cooperativity with which aspartate is recognized by the Tar chemoreceptor (Milligan and Koshland, 1993). Further ITC experiments using 15 compounds that are structurally related to αKG resulted in an absence of binding, indicating that McpK is a αKG specific receptor (Martin-Mora *et al*., 2016b). The existence of a αKG-specific receptor may be related to the central metabolic role of this compound. Apart from being part of the tricarboxylic acid (TCA) cycle, it is also a branch point from which other pathways depart such as the GABA shunt or routes for the synthesis of purine, pyrimidines, coenzyme B or several amino acids.

• *D/L-Asp and L-Glu.* Chemoreceptors with a dCACHE LBD appear to be the primary family for chemotaxis to amino acids (Reyes-Darias *et al*., 2015a). Characterized family members comprise, for example, broad range amino acid receptors in *Bacillus subtilis* (Glekas *et al*., 2012), *Sinorhizobium* (*Ensifer*) *meliloti* (Webb *et al*., 2017a), *P. putida* (Corral-Lugo *et al*., 2016) and *P. aeruginosa* (Taguchi *et al*., 1997; Rico-Jimenez *et al*., 2013) or more specific receptors with preference for Gln (Rico-Jimenez *et al*., 2013), Asn (Glekas *et al*., 2010) or Arg (Feng *et al*., 2018). TSA and ITC were central to characterize the PscA chemoreceptor of different pathovars of the plant pathogen *P. syringae*. PscA-LBD specifically binds D/L-Asp and L-Glu (McKellar *et al*., 2015; Cerna-Vargas *et al*., 2019) with affinities ranging between 1.2 and 3.4 µM (Cerna-Vargas *et al*., 2019). Interestingly, Asp and Glu are the most abundant proteinogenic amino acids in plants (Kumar *et al*., 2017), a fact that may explain the evolution of an Asp- and Glu-specific chemoreceptor in plant pathogens. Chemotaxis to compounds released from the plant stomata is thought to facilitate bacterial plant entry (Matilla and Krell, 2018) and the presence of D-Asp, an enantiomer that cannot be

metabolized by *P. syringae*, was found to reduce virulence in this phytopathogen (Cerna-Vargas *et al*., 2019).

• *Short-chain carboxylic acids.* The discovery of the homologous chemoreceptors for short-chain carboxylic acids in *P. putida*, *P. syringae* and *S. meliloti* is largely due to LBD-based ligand screening (Garcia *et al*., 2015; Brewster *et al*., 2016; Compton *et al*., 2018). The common feature of these receptors is their sCACHE type LBD. The ligand profiles of these three chemoreceptors were different but overlapping and include a number of carboxylic acids that harbour primarily two or three carbon atoms. A common feature of all three receptors is the binding with significant affinity of acetate (K_D 9.1–34 μM) that also cause important chemotactic responses indicative of being the ligand with primary relevance.

• *Evidence for chemoreceptor signal antagonists.* Protein-based ligand screening has been central to the identification of signal antagonists, i.e., compounds that bind to the chemoreceptor LBD but do not cause downstream signalling. Malate is a strong chemoattractant for *P. aeruginosa* and the corresponding chemoreceptor has been identified (Alvarez-Ortega and Harwood, 2007). LBD-based ligand screening identified four additional ligands of this receptor, namely bromosuccinic, citramalic, methylsuccinic and citraconic acids (Martin-Mora *et al*., 2018a). However, only the former two compounds triggered chemotaxis, whereas the latter two compounds, termed antagonists, were found to compete with the chemoattractants for binding but did not cause any significant response on its own. Importantly, the presence of increasing concentrations of antagonists reduced the magnitude of malate chemotaxis (Martin-Mora *et al*., 2018a). Evidence for signal antagonists have also been obtained previously for the Tar chemoreceptor (Bi *et al*., 2013), two-component systems (Busch *et al*., 2007) and transcriptional regulators (Matilla *et al*., 2018). Antagonists may thus correspond to a more general phenomenon in bacterial signal transduction.

Use of microcalorimetry to characterize ligand binding at novel chemoreceptors. In a number of cases, novel chemoreceptors have been identified by studying chemotaxis of chemoreceptor mutants. In subsequent studies, ITC has proven to be essential to determine whether ligand binding occurs directly or via a ligand-binding protein. Frequently, binding constants derived by ITC have identified ligands that are preferentially recognized providing interesting insight into forces that have led to chemoreceptor evolution in a particular habitat. Listed below are some representative examples.

• *Quaternary amines.* Analyses of alfalfa seed exudates led to the identification of quaternary ammonium compounds as abundant constituents and *S. meliloti* showed chemoattraction to these compounds (Webb *et al*., 2017b). Chemotaxis assays with chemoreceptor mutants identified McpX as the corresponding chemoreceptor. TSAs have then been used to demonstrate that these compounds bind directly to the LBD and ITC experiments revealed that this receptor has a strong ligand preference for choline, which is the most abundant quaternary amine in seed exudates (Webb *et al*., 2017b).

• *Taurine.* Taurine is a major bile component and abundant in the intestine of humans and other vertebrates. *Vibrio cholerae*, the etiological agent of cholera, was found to possess a chemoreceptor with a dCACHE domain, Mlp37, that mediates chemotaxis to taurine (Nishiyama *et al*., 2016). In the presence of taurine, Mlp37 became methylated and ITC of the Mlp37-LBD was essential to demonstrate that this receptor binds taurine directly (K_D = 3.2 μM), but also a number of amino acids with similar affinity.

• *Boric acid.* In analogy to the above studies, chemotaxis assays with chemoreceptor mutants of the phytopathogen *Ralstonia pseudosolanacearum* identified a chemoreceptor for boric acid, termed McpB. Boron serves as a micronutrient in prokaryotes and is required for the synthesis of a number of biologically active borate containing compounds (Rezanka and Sigler, 2008). Microcalorimetric titrations showed that boric acid binds directly to the individual 4HB LBD with a K_D of 5.4 μM (Hida *et al*., 2017). The derived n value suggested a one ligand per LBD dimer stoichiometry, similar to Tar (Milligan and Koshland, 1993); a finding that was verified by analytical ultracentrifugation (Hida *et al*., 2017).

• *Inorganic phosphate. Pseudomonas aeruginosa* shows strong chemotaxis to inorganic phosphate (Pi), which is a central signal molecule controlling the expression of virulence related genes (Zaborin *et al*., 2009; Bains *et al*., 2012). Chemotaxis experiments revealed that a mutant defective in the CtpH chemoreceptor failed to respond to high Pi concentrations, whereas a mutant in the CtpL chemoreceptor did not respond to low Pi concentrations (Wu *et al*., 2000). Microcalorimetric titrations showed that CtpH-LBD bound preferentially Pi and in addition several pyrophosphate containing compounds with lower affinity (Rico-Jimenez *et al*., 2016). In contrast, CtpL-LBD failed to bind Pi, a finding that has motivated studies to identify potential periplasmic ligand-binding proteins. Pull-down experiments permitted the identification of Pi loaded PstS as the CtpL-LBD ligand (Rico-Jimenez *et al*., 2016). PstS is the periplasmic Pi

binding protein that provides the substrate to the PstABC transporter (Nikata *et al*., 1996). Further ITC studies showed that PstS binds Pi with a K_D of 7 nM, representing ultratight binding that is related to the capacity of the receptor to respond to low Pi concentrations (Rico-Jimenez *et al*., 2016).

So far, chemoreceptors for three important inorganic anions have been identified, namely nitrate, borate and inorganic phosphate. Common features of the corresponding chemoreceptors, McpN, McpB, CtpH and CtpL, include their high ligand specificity and the four helix bundle architecture of the corresponding LBDs (Rico-Jimenez *et al*., 2016; Hida *et al*., 2017; Martin-Mora *et al*., 2019).

• *Citrate.* The saprophytic *P. putida* KT2440 was shown to possess with McpS a chemoreceptor for most TCA cycle intermediates (Lacal *et al*., 2010; Pineda-Molina *et al*., 2012). McpS is the first characterized member of the chemoreceptor family with a HBM domain (Ortega and Krell, 2014). Microcalorimetric titrations resulted in a stoichiometry of one ligand per LBD dimer (Pineda-Molina *et al*., 2012) that corresponds thus to the same stoichiometry as the Tar chemoreceptor (Milligan and Koshland, 1993). Citrate is abundantly present in plant tissues and root exudates, where it is primarily complexed with bivalent cations like Mg^{2+}. However, ITC studies showed that McpS-LBD only recognized free citrate with low affinity and failed to bind citrate in complex with physiologically relevant metal ions (Lacal *et al*., 2011). Considering the physiological relevance of citrate, it was hypothesized that there may be another receptor that mediates citrate chemotaxis. The research undertaken led to the identification of the HBM domain containing chemoreceptor McpQ that was shown by ITC to bind exclusively citrate either in its free or metal bound form (Martin-Mora *et al*., 2016a). Interestingly, the affinity of metal-bound citrate was superior to that of free citrate (Martin-Mora *et al*., 2016a), a finding that may reflect the presence of primarily metal bound citrate in the environment.

• Cis-*aconitate.* The intermediate following citrate in the TCA cycle is *cis*-aconitate. A mutant of the MCP2983 chemoreceptor from *Comamonas testosteroni* failed to mediate chemotaxis to a series of carboxylic acids and aromatic compounds (Ni *et al*., 2015). However, microcalorimetric titrations of the MCP2983-LBD (4HB) showed that *cis*-aconitate is the only compound recognized. To explain the discrepancy between the specificity of ligand recognition and the broad range of chemotaxis mediated by this receptor, the authors argue that the metabolism of different chemoeffectors results in *cis*-aconitate that in turn is recognized by the chemoreceptor producing this broad chemotactic response (Ni *et al*., 2015).

Taken together, microcalorimetry was essential to document the existence of chemoreceptors that recognize preferentially or exclusively a single TCA cycle intermediate, namely citrate (Martin-Mora *et al*., 2016a), *cis*-aconitate (Ni *et al*., 2015), α-ketoglutarate (Martin-Mora *et al*., 2016b) and malate (33,57), indicating the central physiological relevance of these compounds for a broad range of bacteria.

Relating system input and output. Signal transduction processes involve the conversion of an input into an output. The dissociation constant of a ligand to a chemoreceptor LBD is a measure of the signalling input. A remarkable characteristic of an ITC analysis is the precision with which K_D values can be determined. On the other hand, fluorescence resonance energy transfer (FRET) measurements using cells with fluorescent labelled CheY and CheZ is an approach that permits a very precise definition of the signalling output (Paulick and Sourjik, 2018). The combination of both approaches has provided interesting insight into chemoreceptor function.

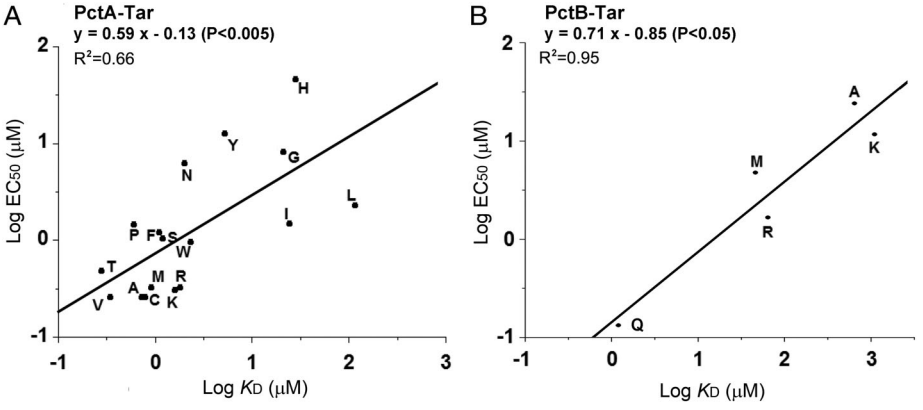

Fig 5 Relationship between signalling input and output for the PctA (A) and PctB (B) chemoreceptors. Signalling input is represented by the K_D values determined by microcalorimetric titrations of individual LBDs. Signalling output corresponds to the EC_{50} values derived from FRET measurements of chemoreceptor chimera combining the PctA or PctB LBDs of *P. aeruginosa* PAO1 with the *E. coli* Tar signalling domain. Figure reproduced with permission from Reyes-Darias *et al*. (2015a).

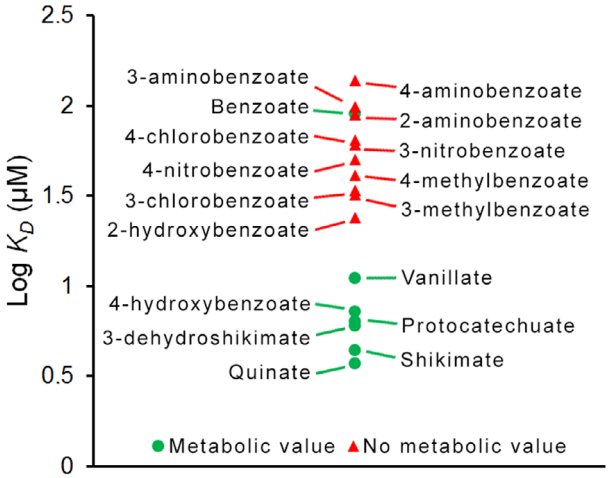

Fig 6 Relationship between chemoreceptor affinity and metabolic value of chemoattractants. Binding of ligands to the LBD of the PcaY_PP chemoreceptor of *P. putida* KT2440. Shown are K_D values as derived by microcalorimetric titrations and the colour indicates the metabolic value. Data taken from Fernandez *et al*. (2017). [Color figure can be viewed at wileyonlinelibrary.com]

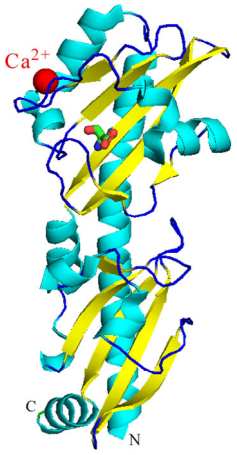

Mlp24-LBD
(+Ca^{2+} and serine)

Fig 7 Three dimensional structure of a chemoreceptor ligand binding domain with multiple bound ligands. LBD of Mlp24 chemoreceptor of *V. cholerae* O395N1 in complex with serine and Ca^{2+} (PDB ID: 6IOU). [Color figure can be viewed at wileyonlinelibrary.com]

dCACHE domains are extremely abundant in bacteria and present in all major prokaryotic signal transduction families that rely on extracytoplasmic sensing (Upadhyay *et al*., 2016). In addition, almost one third of all chemoreceptors possess a CACHE domain (Ortega *et al*., 2017a). The three paralogous chemoreceptors PctA, PctB and PctC of *P. aeruginosa* can be considered as models to study dCACHE-containing chemoreceptors (Taguchi *et al*., 1997; Schmidt *et al*., 2011; Rico-Jimenez *et al*., 2013; McKellar *et al*., 2015; Xu *et al*., 2016; Corral-Lugo *et al*., 2018; Gavira *et al*., 2020). PctA and PctB recognize 17 and 5 amino acids respectively (Rico-Jimenez *et al*., 2013). To determine the signalling output of both receptors, chimeric receptors were produced that contain the PctA or PctB LBD fused to the Tar signalling domain. These chimeras were introduced into a chemoreceptor-free *E. coli* strain and responses measured in function of different concentrations of each of the ligands, leading to the determination of EC_{50} values (Reyes-Darias *et al*., 2015a). Interestingly, these EC_{50} values correlated with K_D values as determined by ITC, representing the signalling input (Fig. 5). There was thus a correlation between the magnitude of signal input and output, indicating that the onset of binding determines the onset of response (Reyes-Darias *et al*., 2015a). Further studies are necessary to determine to what degree these findings apply to other chemoreceptors.

Metabolic value has shaped chemoreceptor evolution. Studies of *E. coli* have shown that chemotaxis occurs preferentially to amino acids that are rapidly consumed, indicating that the nutritional value of a ligand has shaped chemotaxis (Yang *et al*., 2015). To elucidate potential molecular mechanisms of this preference, we have conducted studies of the PcaY_PP chemoreceptor of *P. putida* KT2440 (Fernandez *et al*., 2017). This receptor and its homologue in *P. putida* F1 (Luu *et al*., 2015) were found respond to a wide range of C6 ring containing carboxylic acids of which only some are of apparent metabolic value, as indicated by their capacity to support bacterial growth as sole carbon source.

Microcalorimetric titrations of PcaY_PP-LBD revealed binding of 17 compounds, with K_D values between 3.7 and 138 μM (Fernandez *et al*., 2017). All compounds induced chemotaxis but only seven of these compounds were of metabolic value (Fernandez *et al*., 2017). However, the affinities of metabolic value compounds were in general significantly higher than those of no metabolic value compounds (Fig. 6). These data suggest that the nutritional value of a compound has shaped molecular recognition during chemoreceptor evolution. The most tightly binding ligand was quinate which is a very abundant carbon storage compound in plants (Lehmann *et al*., 2016) and chemotaxis of saprophytic *P. putida* KT2440 to this compound may represent a significant benefit.

Binding of multiple ligands to chemoreceptor LBDs. The Mlp24 chemoreceptor of *V. cholerae* was shown to mediate chemotaxis to a series of amino acids (Nishiyama *et al*., 2012). When the 3D structures of Mlp24-LBD in complex with different amino acids were inspected, a Ca^{2+} ion was bound to a loop next to the amino acid binding pocket (Takahashi *et al*., 2019) (Fig. 7). Chemotaxis experiments showed that Ca^{2+} binding does not trigger

chemotaxis and microcalorimetry played an essential role to determine the relevance of Ca^{2+} binding for the functioning of this receptor. Thus, when Mlp24-LBD was titrated with different amino acids in the absence and presence of saturating Ca^{2+} concentrations, the authors noted a significant increase in affinity for some but not all amino acids in the presence of Ca^{2+}; a finding that was also reflected in an increase in the magnitude of chemotaxis to some of the amino acids. *V. cholerae* is present in seawaters and colonizes the intestine, niches that contain approximately 10 mM Ca^{2+}. As a result, the authors suggest that Ca^{2+} corresponds to a physiologically relevant co-signal that modulates the affinity for the primary amino acid signal (Takahashi *et al*., 2019). Further studies will show whether the existence of co-signals is a more general phenomenon in chemoreceptors.

Conclusions

Chemosensory systems are often highly complex since they involve many signalling proteins, which are frequently organized in multiple pathways that exert different cellular functions. Furthermore, a single bacterial genome can encode a large number of chemoreceptors that at times possess overlapping ligand specificities and the significant sequence divergence of LBDs hampers chemoreceptor annotation by homology with characterized receptors. These issues represent a significant challenge to the scientific community since the identification of the signal molecules recognized by specific chemoreceptors is key to understand their physiological role(s). ITC has been shown to be a very potent tool to tackle some of these challenges. Importantly, the fact that most LBDs can be produced in significant amounts as individual proteins that maintain ligand-binding properties has potentiated the role of ITC in the identification of many novel chemoreceptors. The major limitations of a traditional microcalorimetric analysis are the requirement of significant amounts of protein and its labour intensity. However, microcalorimetric technology is advancing rapidly and last generation instruments require much less protein. In addition, automated instruments that conduct experiments and analyse data in an almost autonomous manner are now available. This, and the fact that the approach used to study chemoreceptors can also be applied to other signal transduction systems will enhance the importance of microcalorimetry in laboratories studying prokaryotic signal transduction.

Acknowledgements

This work was supported by FEDER funds and Fondo Social Europeo through grant BIO2016-76779-P from the Spanish Ministry for Economy and Competitiveness to TK.

References

Alvarez-Ortega, C., and Harwood, C.S. (2007) Identification of a malate chemoreceptor in *Pseudomonas aeruginosa* by screening for chemotaxis defects in an energy taxis-deficient mutant. *Appl Environ Microbiol* **73**: 7793–7795.

Bains, M., Fernandez, L., and Hancock, R.E. (2012) Phosphate starvation promotes swarming motility and cytotoxicity of *Pseudomonas aeruginosa*. *Appl Environ Microbiol* **78**: 6762–6768.

Baraquet, C., and Harwood, C.S. (2013) Cyclic diguanosine monophosphate represses bacterial flagella synthesis by interacting with the Walker a motif of the enhancer-binding protein FleQ. *Proc Natl Acad Sci U S A* **110**: 18478–18483.

Bardy, S.L., Briegel, A., Rainville, S., and Krell, T. (2017) Recent advances and future prospects in bacterial and archaeal locomotion and signal transduction. *J Bacteriol* **199**: e00203–e00217.

Barnakov, A.N., Barnakova, L.A., and Hazelbauer, G.L. (1999) Efficient adaptational demethylation of chemoreceptors requires the same enzyme-docking site as efficient methylation. *Proc Natl Acad Sci U S A* **96**: 10667–10672.

Bartelli, N.L., and Hazelbauer, G.L. (2011) Direct evidence that the carboxyl-terminal sequence of a bacterial chemoreceptor is an unstructured linker and enzyme tether. *Protein Sci* **20**: 1856–1866.

Bi, S., and Sourjik, V. (2018) Stimulus sensing and signal processing in bacterial chemotaxis. *Curr Opin Microbiol* **45**: 22–29.

Bi, S., Yu, D., Si, G., Luo, C., Li, T., Ouyang, Q., *et al*. (2013) Discovery of novel chemoeffectors and rational design of *Escherichia coli* chemoreceptor specificity. *Proc Natl Acad Sci U S A* **110**: 16814–16819.

Bjorkman, A.M., Dunten, P., Sandgren, M.O., Dwarakanath, V.N., and Mowbray, S.L. (2001) Mutations that affect ligand binding to the *Escherichia coli* aspartate receptor: implications for transmembrane signaling. *J Biol Chem* **276**: 2808–2815.

Boehm, A., Kaiser, M., Li, H., Spangler, C., Kasper, C.A., Ackermann, M., *et al*. (2010) Second messenger-mediated adjustment of bacterial swimming velocity. *Cell* **141**: 107–116.

Brewster, J.L., McKellar, J.L., Finn, T.J., Newman, J., Peat, T.S., and Gerth, M.L. (2016) Structural basis for ligand recognition by a cache chemosensory domain that mediates carboxylate sensing in *Pseudomonas syringae*. *Sci Rep* **6**: 35198.

Briegel, A., Li, X., Bilwes, A.M., Hughes, K.T., Jensen, G.J., and Crane, B.R. (2012) Bacterial chemoreceptor arrays are hexagonally packed trimers of receptor dimers networked by rings of kinase and coupling proteins. *Proc Natl Acad Sci U S A* **109**: 3766–3771.

Briegel, A., Ortega, D.R., Mann, P., Kjaer, A., Ringgaard, S., and Jensen, G.J. (2016) Chemotaxis cluster 1 proteins form cytoplasmic arrays in *Vibrio cholerae* and are stabilized by a double signaling domain receptor DosM. *Proc Natl Acad Sci U S A* **113**: 10412–10417.

Busch, A., Lacal, J., Martos, A., Ramos, J.L., and Krell, T. (2007) Bacterial sensor kinase TodS interacts with agonistic and antagonistic signals. *Proc Natl Acad Sci U S A* **104**: 13774–13779.

Cerna-Vargas, J.P., Santamaria-Hernando, S., Matilla, M.A., Rodriguez-Herva, J.J., Daddaoua, A., Rodriguez-Palenzuela, P., *et al*. (2019) Chemoperception of specific amino acids controls Phytopathogenicity in *Pseudomonas syringae* pv. Tomato. *MBio* **10**: e01868–e01819.

Chiu, M.H., and Prenner, E.J. (2011) Differential scanning calorimetry: an invaluable tool for a detailed thermodynamic characterization of macromolecules and their interactions. *J Pharm Bioallied Sci* **3**: 39–59.

Clarke, S., and Koshland, D.E., Jr. (1979) Membrane receptors for aspartate and serine in bacterial chemotaxis. *J Biol Chem* **254**: 9695–9702.

Compton, K.K., Hildreth, S.B., Helm, R.F., and Scharf, B.E. (2018) *Sinorhizobium meliloti* chemoreceptor McpV senses short chain carboxylates via direct binding. *J Bacteriol* **200**: e00519–e00518.

Corral-Lugo, A., de la Torre, J., Matilla, M.A., Fernandez, M., Morel, B., Espinosa-Urgel, M., and Krell, T. (2016) Assessment of the contribution of chemoreceptor-based signaling to biofilm formation. *Environ Microbiol* **18**: 3355–3372.

Corral-Lugo, A., Matilla, M.A., Martin-Mora, D., Silva Jimenez, H., Mesa Torres, N., Kato, J., *et al*. (2018) High-affinity chemotaxis to histamine mediated by the TlpQ chemoreceptor of the human pathogen *Pseudomonas aeruginosa*. *MBio* **9**: e01894–e01818.

Du, X., Kong, K., Tang, H., Tang, H., Jiao, X., and Huang, J. (2018) The novel protein Cj0371 inhibits chemotaxis of *Campylobacter jejuni*. *Front Microbiol* **9**: 1904.

Ehrhardt, M.K.G., Warring, S.L., and Gerth, M.L. (2018) Screening chemoreceptor-ligand interactions by high-throughput thermal-shift assays. *Methods Mol Biol* **1729**: 281–290.

Feng, H., Zhang, N., Du, W., Zhang, H., Liu, Y., Fu, R., *et al*. (2018) Identification of chemotaxis compounds in root exudates and their sensing chemoreceptors in plant growth-promoting rhizobacteria *Bacillus amyloliquefaciens* SQR9. *Mol Plant Microbe Interact* **31**: 995–1005.

Fernandez, M., Morel, B., Corral-Lugo, A., and Krell, T. (2016) Identification of a chemoreceptor that specifically mediates chemotaxis toward metabolizable purine derivatives. *Mol Microbiol* **99**: 34–42.

Fernandez, M., Matilla, M.A., Ortega, A., and Krell, T. (2017) Metabolic value Chemoattractants are preferentially recognized at broad ligand range chemoreceptor of *Pseudomonas putida* KT2440. *Front Microbiol* **8**: 990.

Fernandez, M., Ortega, A., Rico-Jimenez, M., Martin-Mora, D., Daddaoua, A., Matilla, M.A., and Krell, T. (2018) High-throughput screening to identify chemoreceptor ligands. *Methods Mol Biol* **1729**: 291–301.

Fernández, M., Morel, B., Corral-Lugo, A., Rico-Jiménez, M., Martín-Mora, D., López-Farfán, D., *et al*. (2016) Identification of ligands for bacterial sensor proteins. *Curr Genet* **62**: 143–147.

Fulcher, N.B., Holliday, P.M., Klem, E., Cann, M.J., and Wolfgang, M.C. (2010) The *Pseudomonas aeruginosa* Chp chemosensory system regulates intracellular cAMP levels by modulating adenylate cyclase activity. *Mol Microbiol* **76**: 889–904.

Garcia-Fontana, C., Corral Lugo, A., and Krell, T. (2014) Specificity of the CheR2 methyltransferase in *Pseudomonas aeruginosa* is directed by a C-terminal pentapeptide in the McpB chemoreceptor. *Sci Signal* **7**: ra34.

Garcia-Fontana, C., Reyes-Darias, J.A., Munoz-Martinez, F., Alfonso, C., Morel, B., Ramos, J.L., and Krell, T. (2013) High specificity in CheR methyltransferase function: CheR2 of *Pseudomonas putida* is essential for chemotaxis, whereas CheR1 is involved in biofilm formation. *J Biol Chem* **288**: 18987–18999.

Garcia, V., Reyes-Darias, J.A., Martin-Mora, D., Morel, B., Matilla, M.A., and Krell, T. (2015) Identification of a chemoreceptor for C2 and C3 carboxylic acids. *Appl Environ Microbiol* **81**: 5449–5457.

Gavira, J.A., Gumerov, V.M., Rico-Jimenez, M., Petukh, M., Upadhyay, A.A., Ortega, A., *et al*. (2020) How bacterial chemoreceptors evolve novel ligand specificities. *mBio* **11**: e03066–e03019.

Glekas, G.D., Foster, R.M., Cates, J.R., Estrella, J.A., Wawrzyniak, M.J., Rao, C.V., and Ordal, G.W. (2010) A PAS domain binds asparagine in the chemotaxis receptor McpB in *Bacillus subtilis*. *J Biol Chem* **285**: 1870–1878.

Glekas, G.D., Mulhern, B.J., Kroc, A., Duelfer, K.A., Lei, V., Rao, C.V., and Ordal, G.W. (2012) The *Bacillus subtilis* chemoreceptor McpC senses multiple ligands using two discrete mechanisms. *J Biol Chem* **287**: 39412–39418.

Gumerov, V.M., Ortega, D.R., Adebali, O., Ulrich, L.E., and Zhulin, I.B. (2020) MiST 3.0: an updated microbial signal transduction database with an emphasis on chemosensory systems. *Nucleic Acids Res* **48**: D459–D464.

Hanlon, D.W., and Ordal, G.W. (1994) Cloning and characterization of genes encoding methyl-accepting chemotaxis proteins in *Bacillus subtilis*. *J Biol Chem* **269**: 14038–14046.

Hickman, J.W., and Harwood, C.S. (2008) Identification of FleQ from *Pseudomonas aeruginosa* as a c-di-GMP-responsive transcription factor. *Mol Microbiol* **69**: 376–389.

Hickman, J.W., Tifrea, D.F., and Harwood, C.S. (2005) A chemosensory system that regulates biofilm formation through modulation of cyclic diguanylate levels. *Proc Natl Acad Sci U S A* **102**: 14422–14427.

Hida, A., Oku, S., Nakashimada, Y., Tajima, T., and Kato, J. (2017) Identification of boric acid as a novel chemoattractant and elucidation of its chemoreceptor in *Ralstonia pseudosolanacearum* Ps29. *Sci Rep* **7**: 8609.

Hou, Y.J., Yang, W.S., Hong, Y., Zhang, Y., Wang, D.C., and Li, D.F. (2020) Structural insights into the mechanism of c-di-GMP-bound YcgR regulating flagellar motility in *Escherichia coli*. *J Biol Chem* **295**: 808–821.

Huang, Z., Ni, B., Jiang, C.Y., Wu, Y.F., He, Y.Z., Parales, R.E., and Liu, S.J. (2016) Direct sensing and signal transduction during bacterial chemotaxis toward aromatic compounds in *Comamonas testosteroni*. *Mol Microbiol* **101**: 224–237.

Jenal, U., Reinders, A., and Lori, C. (2017) Cyclic di-GMP: second messenger extraordinaire. *Nat Rev Microbiol* **15**: 271–284.

Jones, C.W., and Armitage, J.P. (2017) Essential role of the cytoplasmic chemoreceptor TlpT in the De novo formation of chemosensory complexes in *Rhodobacter sphaeroides*. *J Bacteriol* **199**: e00366–e00317.

Krainer, G., and Keller, S. (2015) Single-experiment displacement assay for quantifying high-affinity binding by isothermal titration calorimetry. *Methods* **76**: 116–123.

Krell, T. (2008) Microcalorimetry: a response to challenges in modern biotechnology. *J Microbial Biotechnol* **1**: 126–136.

Kumar, V., Sharma, A., Kaur, R., Thukral, A.K., Bhardwaj, R., and Ahmad, P. (2017) Differential distribution of amino acids in plants. *Amino Acids* **49**: 821–869.

Lacal, J., Garcia-Fontana, C., Callejo-Garcia, C., Ramos, J. L., and Krell, T. (2011) Physiologically relevant divalent cations modulate citrate recognition by the McpS chemoreceptor. *J Mol Recognit* **24**: 378–385.

Lacal, J., Alfonso, C., Liu, X., Parales, R.E., Morel, B., Conejero-Lara, F., *et al*. (2010) Identification of a chemoreceptor for tricarboxylic acid cycle intermediates: differential chemotactic response towards receptor ligands. *J Biol Chem* **285**: 23126–23136.

Ladbury, J.E. (2010) Calorimetry as a tool for understanding biomolecular interactions and an aid to drug design. *Biochem Soc Trans* **38**: 888–893.

Lehmann, M.M., Wegener, F., Werner, R.A., and Werner, C. (2016) Diel variations in carbon isotopic composition and concentration of organic acids and their impact on plant dark respiration in different species. *Plant Biol (Stuttg)* **18**: 776–784.

Lertsethtakarn, P., Howitt, M.R., Castellon, J., Amieva, M.R., and Ottemann, K.M. (2015) *Helicobacter pylori* CheZ(HP) and ChePep form a novel chemotaxis-regulatory complex distinct from the core chemotaxis signaling proteins and the flagellar motor. *Mol Microbiol* **97**: 1063–1078.

Li, M., and Hazelbauer, G.L. (2006) The carboxyl-terminal linker is important for chemoreceptor function. *Mol Microbiol* **60**: 469–479.

Li, M., and Hazelbauer, G.L. (2020) Methyltransferase CheR binds to its chemoreceptor substrates independent of their signaling conformation yet modifies them differentially. *Protein Sci* **29**: 443–454.

Li, R., Gu, J., Chen, Y.Y., Xiao, C.L., Wang, L.W., Zhang, Z. P., *et al*. (2010) CobB regulates *Escherichia coli* chemotaxis by deacetylating the response regulator CheY. *Mol Microbiol* **76**: 1162–1174.

Lin, L.N., Li, J., Brandts, J.F., and Weis, R.M. (1994) The serine receptor of bacterial chemotaxis exhibits half-site saturation for serine binding. *Biochemistry* **33**: 6564–6570.

Liu, Y.C., Machuca, M.A., Beckham, S.A., Gunzburg, M.J., and Roujeinikova, A. (2015) Structural basis for amino-acid recognition and transmembrane signalling by tandem per-Arnt-Sim (tandem PAS) chemoreceptor sensory domains. *Acta Crystallogr D Biol Crystallogr* **71**: 2127–2136.

Luu, R.A., Kootstra, J.D., Nesteryuk, V., Brunton, C.N., Parales, J.V., Ditty, J.L., and Parales, R.E. (2015) Integration of chemotaxis, transport and catabolism in *Pseudomonas putida* and identification of the aromatic acid chemoreceptor PcaY. *Mol Microbiol* **96**: 134–147.

Machuca, M.A., Johnson, K.S., Liu, Y.C., Steer, D.L., Ottemann, K.M., and Roujeinikova, A. (2017) *Helicobacter pylori* chemoreceptor TlpC mediates chemotaxis to lactate. *Sci Rep* **7**: 14089.

Martin-Mora, D., Ortega, A., Perez-Maldonado, F.J., Krell, T., and Matilla, M.A. (2018a) The activity of the C4-dicarboxylic acid chemoreceptor of *Pseudomonas aeruginosa* is controlled by chemoattractants and antagonists. *Sci Rep* **8**: 2102.

Martin-Mora, D., Reyes-Darias, J.A., Ortega, A., Corral-Lugo, A., Matilla, M.A., and Krell, T. (2016a) McpQ is a specific citrate chemoreceptor that responds preferentially to citrate/metal ion complexes. *Environ Microbiol* **18**: 3284–3295.

Martin-Mora, D., Ortega, A., Matilla, M.A., Martinez-Rodriguez, S., Gavira, J.A., and Krell, T. (2019) The molecular mechanism of nitrate chemotaxis via direct ligand binding to the PilJ domain of McpN. *MBio* **10**: e02334–e02318.

Martin-Mora, D., Ortega, A., Reyes-Darias, J.A., García, V., López-Farfán, D., Matilla, M.A., and Krell, T. (2016b) Identification of a chemoreceptor in *Pseudomonas aeruginosa* that specifically mediates chemotaxis towards alpha-ketoglutarate. *Front Microbiol* **7**: 1937.

Martin-Mora, D., Fernandez, M., Velando, F., Ortega, A., Gavira, J.A., Matilla, M.A., and Krell, T. (2018b) Functional annotation of bacterial signal transduction systems: Progress and challenges. *Int J Mol Sci* **19**: 3755.

Matilla, M.A., and Krell, T. (2017) Chemoreceptor-based signal sensing. *Curr Opin Biotechnol* **45**: 8–14.

Matilla, M.A., and Krell, T. (2018) The effect of bacterial chemotaxis on host infection and pathogenicity. *FEMS Microbiol Rev* **42**, 40–67. https://doi.org/10.1093/femsre/fux1052.

Matilla, M.A., Daddaoua, A., Chini, A., Morel, B., and Krell, T. (2018) An auxin controls bacterial antibiotics production. *Nucleic Acids Res* **46**: 11229–11238.

McKellar, J.L., Minnell, J.J., and Gerth, M.L. (2015) A high-throughput screen for ligand binding reveals the specificities of three amino acid chemoreceptors from *Pseudomonas syringae* pv. *actinidiae*. *Mol Microbiol* **96**: 694–707.

Milligan, D.L., and Koshland, D.E., Jr. (1993) Purification and characterization of the periplasmic domain of the aspartate chemoreceptor. *J Biol Chem* **268**: 19991–19997.

Ni, B., Huang, Z., Fan, Z., Jiang, C.Y., and Liu, S.J. (2013) *Comamonas testosteroni* uses a chemoreceptor for tricarboxylic acid cycle intermediates to trigger chemotactic responses towards aromatic compounds. *Mol Microbiol* **90**: 813–823.

Ni, B., Huang, Z., Wu, Y.F., Fan, Z., Jiang, C.Y., and Liu, S. J. (2015) A novel chemoreceptor MCP2983 from *Comamonas testosteroni* specifically binds to *cis*-aconitate and triggers chemotaxis towards diverse organic compounds. *Appl Microbiol Biotechnol* **99**: 2773–2781.

Nikata, T., Sakai, Y., Shibat, K., Kato, J., Kuroda, A., and Ohtake, H. (1996) Molecular analysis of the phosphate-specific transport (*pst*) operon of *Pseudomonas aeruginosa*. *Mol Gen Genet* **250**: 692–698.

Nishiyama, S., Suzuki, D., Itoh, Y., Suzuki, K., Tajima, H., Hyakutake, A., *et al*. (2012) Mlp24 (McpX) of *Vibrio cholerae* implicated in pathogenicity functions as a chemoreceptor for multiple amino acids. *Infect Immun* **80**: 3170–3178.

Nishiyama, S., Takahashi, Y., Yamamoto, K., Suzuki, D., Itoh, Y., Sumita, K., *et al*. (2016) Identification of a *Vibrio cholerae* chemoreceptor that senses taurine and amino acids as attractants. *Sci Rep* **6**: 20866.

Ortega, A., and Krell, T. (2014) The HBM domain: introducing bimodularity to bacterial sensing. *Protein Sci* **23**: 332–336.

Ortega, A., Zhulin, I.B., and Krell, T. (2017a) Sensory repertoire of bacterial chemoreceptors. *Microbiol Mol Biol Rev* **81**: e00033–00017.

Ortega, D.R., Fleetwood, A.D., Krell, T., Harwood, C.S., Jensen, G.J., and Zhulin, I.B. (2017b) Assigning chemoreceptors to chemosensory pathways in *Pseudomonas aeruginosa*. *Proc Natl Acad Sci U S A* **114**: 12809–12814.

Ortega, D.R., Subramanian, P., Mann, P., Kjær, A., Chen, S., Watts, K.J., *et al*. (2020) Repurposing a chemosensory macromolecular machine. *Nat. Commun.* **11**, 2041. doi.org/10.1101/653600.

Parales, R.E., Luu, R.A., Chen, G.Y., Liu, X., Wu, V., Lin, P., *et al*. (2013) *Pseudomonas putida* F1 has multiple chemoreceptors with overlapping specificity for organic acids. *Microbiology* **159**: 1086–1096.

Parkinson, J.S., Hazelbauer, G.L., and Falke, J.J. (2015) Signaling and sensory adaptation in *Escherichia coli* chemoreceptors: 2015 update. *Trends Microbiol* **23**: 257–266.

Paul, K., Nieto, V., Carlquist, W.C., Blair, D.F., and Harshey, R.M. (2010) The c-di-GMP binding protein YcgR controls flagellar motor direction and speed to affect chemotaxis by a "backstop brake" mechanism. *Mol Cell* **38**: 128–139.

Paulick, A., and Sourjik, V. (2018) FRET analysis of the chemotaxis pathway response. *Methods Mol Biol* **1729**: 107–126.

Perez, E., and Stock, A.M. (2007) Characterization of the *Thermotoga maritima* chemotaxis methylation system that lacks pentapeptide-dependent methyltransferase CheR: MCP tethering. *Mol Microbiol* **63**: 363–378.

Pineda-Molina, E., Reyes-Darias, J.A., Lacal, J., Ramos, J. L., Garcia-Ruiz, J.M., Gavira, J.A., and Krell, T. (2012) Evidence for chemoreceptors with bimodular ligand-binding regions harboring two signal-binding sites. *Proc Natl Acad Sci U S A* **109**: 18926–18931.

Rahman, H., King, R.M., Shewell, L.K., Semchenko, E.A., Hartley-Tassell, L.E., Wilson, J.C., *et al*. (2014) Characterisation of a multi-ligand binding chemoreceptor CcmL (Tlp3) of *Campylobacter jejuni*. *PLoS Pathog* **10**: e1003822.

Reyes-Darias, J.A., Yang, Y., Sourjik, V., and Krell, T. (2015a) Correlation between signal input and output in PctA and PctB amino acid chemoreceptor of *Pseudomonas aeruginosa*. *Mol Microbiol* **96**: 513–525.

Reyes-Darias, J.A., Garcia, V., Rico-Jimenez, M., Corral-Lugo, A., Lesouhaitier, O., Juarez-Hernandez, D., *et al*. (2015b) Specific gamma-aminobutyrate chemotaxis in *pseudomonads* with different lifestyle. *Mol Microbiol* **97**: 488–501.

Rezanka, T., and Sigler, K. (2008) Biologically active compounds of semi-metals. *Phytochemistry* **69**: 585–606.

Rico-Jimenez, M., Reyes-Darias, J.A., Ortega, A., Diez Pena, A.I., Morel, B., and Krell, T. (2016) Two different mechanisms mediate chemotaxis to inorganic phosphate in *Pseudomonas aeruginosa*. *Sci Rep* **6**: 28967.

Rico-Jimenez, M., Munoz-Martinez, F., Garcia-Fontana, C., Fernandez, M., Morel, B., Ortega, A., *et al*. (2013) Paralogous chemoreceptors mediate chemotaxis towards protein amino acids and the non-protein amino acid gamma-aminobutyrate (GABA). *Mol Microbiol* **88**: 1230–1243.

Schmidt, J., Musken, M., Becker, T., Magnowska, Z., Bertinetti, D., Moller, S., *et al*. (2011) The *Pseudomonas aeruginosa* chemotaxis methyltransferase CheR1 impacts on bacterial surface sampling. *PLoS One* **6**: e18184.

Simms, S.A., and Subbaramaiah, K. (1991) The kinetic mechanism of S-adenosyl-L-methionine: glutamylmethyltransferase from *Salmonella typhimurium*. *J Biol Chem* **266**: 12741–12746.

Taguchi, K., Fukutomi, H., Kuroda, A., Kato, J., and Ohtake, H. (1997) Genetic identification of chemotactic transducers for amino acids in *Pseudomonas aeruginosa*. *Microbiology* **143**: 3223–3229.

Tajima, H., Imada, K., Sakuma, M., Hattori, F., Nara, T., Kamo, N., *et al*. (2011) Ligand specificity determined by differentially arranged common ligand-binding residues in bacterial amino acid chemoreceptors Tsr and tar. *J Biol Chem* **286**: 42200–42210.

Takahashi, Y., Nishiyama, S.I., Sumita, K., Kawagishi, I., and Imada, K. (2019) Calcium ions modulate amino acid sensing of the chemoreceptor Mlp24 of *Vibrio cholerae*. *J Bacteriol* **201**: e00779–e00718.

Ud-Din, A., Khan, M.F., and Roujeinikova, A. (2020) Broad specificity of amino acid chemoreceptor CtaA of *Pseudomonas fluorescens* is afforded by plasticity of its amphipathic ligand-binding pocket. *Mol Plant Microbe Interact* MPMI10190277R. **33**: 612–623.

Upadhyay, A.A., Fleetwood, A.D., Adebali, O., Finn, R.D., and Zhulin, I.B. (2016) Cache domains that are homologous to, but different from PAS domains comprise the largest superfamily of extracellular sensors in prokaryotes. *PLoS Comput Biol* **12**: e1004862.

Vega, S., Abian, O., and Velazquez-Campoy, A. (2015) A unified framework based on the binding polynomial for characterizing biological systems by isothermal titration calorimetry. *Methods* **76**: 99–115.

Velazquez-Campoy, A., and Freire, E. (2006) Isothermal titration calorimetry to determine association constants for high-affinity ligands. *Nat Protoc* **1**: 186–191.

Webb, B.A., Hildreth, S., Helm, R.F., and Scharf, B.E. (2014) *Sinorhizobium meliloti* chemoreceptor McpU mediates chemotaxis toward host plant exudates through direct proline sensing. *Appl Environ Microbiol* **80**: 3404–3415.

Webb, B.A., Compton, K.K., Del Campo, J.S.M., Taylor, D., Sobrado, P., and Scharf, B.E. (2017a) *Sinorhizobium meliloti* chemotaxis to multiple amino acids is mediated by the chemoreceptor McpU. *Mol Plant Microbe Interact* **30**: 770–777.

Webb, B.A., Karl Compton, K., Castaneda Saldana, R., Arapov, T.D., Keith Ray, W., Helm, R.F., and Scharf, B.E. (2017b) *Sinorhizobium meliloti* chemotaxis to quaternary ammonium compounds is mediated by the chemoreceptor McpX. *Mol Microbiol* **103**: 333–346.

Whitchurch, C.B., Leech, A.J., Young, M.D., Kennedy, D., Sargent, J.L., Bertrand, J.J., *et al*. (2004) Characterization of a complex chemosensory signal transduction system which controls twitching motility in *Pseudomonas aeruginosa*. *Mol Microbiol* **52**: 873–893.

Wu, H., Kato, J., Kuroda, A., Ikeda, T., Takiguchi, N., and Ohtake, H. (2000) Identification and characterization of two chemotactic transducers for inorganic phosphate in *Pseudomonas aeruginosa*. *J Bacteriol* **182**: 3400–3404.

Wu, J., Li, J., Li, G., Long, D.G., and Weis, R.M. (1996) The receptor binding site for the methyltransferase of bacterial chemotaxis is distinct from the sites of methylation. *Biochemistry* **35**: 4984–4993.

Wuichet, K., and Zhulin, I.B. (2010) Origins and diversification of a complex signal transduction system in prokaryotes. *Sci Signal* **3**: ra50.

Xu, L., Xin, L., Zeng, Y., Yam, J.K., Ding, Y., Venkataramani, P., *et al*. (2016) A cyclic di-GMP-binding adaptor protein interacts with a chemotaxis methyltransferase to control flagellar motor switching. *Sci Signal* **9**: ra102.

Xu, Z., Zhang, H., Zhang, X., Jiang, H., Liu, C., Wu, F., *et al*. (2019) Interplay between the bacterial protein deacetylase CobB and the second messenger c-di-GMP. *EMBO J* **38**: e100948.

Yan, X.F., Xin, L., Yen, J.T., Zeng, Y., Jin, S., Cheang, Q. W., *et al*. (2018) Structural analyses unravel the molecular mechanism of cyclic di-GMP regulation of bacterial chemotaxis via a PilZ adaptor protein. *J Biol Chem* **293**: 100–111.

Yang, Y., Hofler, C., Poschet, G., Wirtz, M., Hell, R., and Sourjik, V. (2015) Relation between chemotaxis and consumption of amino acids in bacteria. *Mol Microbiol* **96**: 1272–1282.

Yi, X., and Weis, R.M. (2002) The receptor docking segment and S-adenosyl-L-homocysteine bind independently to the methyltransferase of bacterial chemotaxis. *Biochim Biophys Acta* **1596**: 28–35.

Zaborin, A., Romanowski, K., Gerdes, S., Holbrook, C., Lepine, F., Long, J., *et al*. (2009) Red death in *Caenorhabditis elegans* caused by *Pseudomonas aeruginosa* PAO1. *Proc Natl Acad Sci U S A* **106**: 6327–6332.

Zusman, D.R., Scott, A.E., Yang, Z., and Kirby, J.R. (2007) Chemosensory pathways, motility and development in *Myxococcus xanthus*. *Nat Rev Microbiol* **5**: 862–872.